JOURNAL OF MATERIALS SCIENCE 14 (1979) 2110–2118

A fractographic criterion for subcritical crack-growth boundaries in hot-pressed alumina

H. P. KIRCHNER, R. M. GRUVER
Ceramic Finishing Company, P.O. Box 498, State College, Pennsylvania 16801, USA.

The percent intergranular fracture (PIF) was measured along radii extending from fracture origins in hot-pressed alumina specimens, fractured at various loading rates and temperatures, and plotted versus estimates of stress intensity factors (K_I) at the various crack lengths. Minima in PIF occur at values of K_I that are close to the critical stress intensity factors (K_{IC}) for cleavage on various crystal lattice planes in sapphire. The subcritical crack-growth boundary ($K_I = K_{IC}$ of the polycrystalline material) occurs near the primary minimum in PIF suggesting that this minimum can be used as a criterion for locating this boundary. In addition, it was noted that the polycrystalline K_{IC} (4.2 MPa $m^{1/2}$) is very close to the K_{IC} for fracture on $\{\bar{1}\,\bar{1}\,2\,6\}$ planes which is 4.3 MPa $m^{1/2}$. These observations suggest that critical crack growth begins when increased fracture energy can no longer be absorbed by cleavage on these planes. There is a secondary minimum at $K_I > K_{IC}$ that appears to be associated with the K_{IC} necessary for fracture on combinations of planes selected by the fracture as alternatives to the high fracture-toughness basal plane.

1. Introduction

Development of fracture theories and failure analysis has been handicapped by the lack of fractographic criteria for locating subcritical crack-growth boundaries in fracture surfaces of ceramics. In this paper, such a criterion is described for hot-pressed (H-P) alumina.

It is well known that fracture origins in H-P alumina, when observed in reflected light by optical microscopy, are surrounded by reflecting spots [1, 2]. In fact, observation of these reflecting spots is the most reliable method of locating the fracture origins. The area of intense reflecting spots is related to the fracture stress and rate of loading [3]. In weak specimens or those fractured in delayed fracture, the areas are relatively large. In strong specimens or those fractured by impact, the areas are relatively small. Cleavage regions are observed surrounding flaws at fracture origins in H-P alumina, 96% alumina and H-P silicon nitride [3, 4]. These cleavage regions are associated with subcritical crack growth [4, 5]. These observations led to efforts to relate the reflecting spots in H-P alumina to cleavage and a one-to-one correspondence was observed. Therefore, the reflecting spots and cleavage regions in H-P alumina are associated with subcritical crack growth.

In an investigation of microplastic processes in a dense, coarse grained alumina, Lankford [6–8] was able to associate the acoustic emission recorded during subcritical crack growth with deformation twinning. The twinning process tends to propagate to adjacent grains and leads to microcrack formation. Therefore, twinning is one mechanism by which cleavage regions form in alumina.

The fracture energy of a crack traversing a polycrystalline ceramic is the sum of the fracture energies of the individual fracture events occuring near the crack front. These events include transgranular fracture on various crystal lattice planes in individual crystals having various orientations to the crack front, intergranular fracture on various crystal surfaces at various orientations to the crack front, and fracture of intergranular phases. It is well known that there can be substantial variations in the fracture energies for various crystal-lattice planes of single crystals. Wiederhorn [9, 10] measured the fracture energies (γ_F) for several crystal-lattice planes in sapphire with the results given in Table I. Also included in the table are

0022–2461/79/092110–09 $02.90/0

estimates of the critical stress intensity factors (K_{IC}) for the individual lattice planes calculated using $K_{IC} = (2E\ \gamma_F)^{1/2}$ in which E is Young's modulus which was assumed to be 407 GN m^{-2}. These values of K_{IC} can be compared with K_{IC} for H-P alumina which is about 4.2 MPa m$^{1/2}$ [11]. Becher [12] measured fracture energies in several additional planes showing that the fracture energies drop off rapidly for planes close to the basal (0 0 0 1) plane.

The principal fracture events in H-P alumina ceramics are cleavage on various crystal planes and intergranular fracture on various crystal surfaces. Because of the wide range of K_{IC} values of the individual cleavage events and knowing that cleavage and intergranular fracture are interspersed near the fracture origin, it is reasonable to expect that K_{IC} of the polycrystalline material will be characterized by a particular combination of cleavage and intergranular fracture events. Based on the above information, an attempt was made to relate the stress intensity factors (K_I) during subcritical crack growth to the critical stress intensity factors of the individual fracture events in the individual crystals and to develop a fractographic criterion for subcritical crackgrowth boundaries in H-P alumina.

2. Procedures

The present research was done by fractographic analysis of H-P alumina specimens fractured in earlier investigations. Preparation and testing of these specimens was described previously [4, 5]. The specimens were cylindrical rods about 3.3 mm diameter, with densities ranging from 99.5 to 99.7% theoretical and average grain size in the range 1 to 3 μm. The specimens were fractured in flexure.

The percentages of intergranular and transgranular fracture, along radii extending from the fracture origins, were determined using scanning electron micrographs (1000 or 2000 x) which were taken at intervals along the radii and assembled to form composite photographs of the fracture surfaces. A grid with spaces approximately equal to one grain size and ten spaces wide was prepared. The grid was placed on the composite photograph and the fracture surface at the centre of each grid space was examined and classified as to whether it was intergranular or transgranular, characterizing a path about ten grains wide. This process was repeated for adjoining rows of the grid. The percentages of intergranular and transgranular fracture varied considerably from one row to the next so averages were calculated for each row which included the results of the preceding and following rows to form three-row running averages.

The stress intensity factors were calculated for each row using the following equation for circular surface cracks [13]

$$K_I = \frac{Y}{Z}\sigma_F\,(a)^{1/2} \qquad (1)$$

in which a is the crack depth, σ_F is the fracture stress, Y is a geometrical parameter which has a value of 2 for surface flaws and 1.8 for internal flaws and Z is a flaw-shape parameter which has a value of 1.57 for semicircular cracks. This equation assumes a planar crack. Also, this equation is strictly correct only for delayed fracture specimens for which the applied stress is constant. For specimens fractured by a linearly increasing load, the K_1 values are overestimated at all crack lengths less than the critical crack length because the stress is over-estimated. However, calculations show that almost all of the crack growth occurs in less than the last 10% of the loading time. In this time the applied stress varies by less than 10%. Therefore, the error in the calculated K_1 values is small for most of the crack growth.

Using the information from the procedures described above, curves of K_1 versus % intergranular fracture (PIF) were plotted. In the initial attempts to determine the relationship between K_I and PIF, the results were scattered. There was no consistent relationship between K_{IC} for the individual fracture events and K_{IC} of the polycrystalline material. The problem seemed to arise because of uncertainties in the K_I values. A possible explanation was that in strong specimens in which there is a rapid variation in K_I with (a), small errors in locating the fracture origin were causing large errors in K_I. Therefore, weaker specimens were studied. More subcritical crack growth occurs in weak specimens and in delayed fracture specimens so that there is more gradual variation in fracture features. Also, more accurate K_I estimates could be made with specimens with well-defined flaws at the fracture origins, symmetrical areas of reflecting spots and symmetrical fracture mirrors. Therefore, specimens with these characteristics

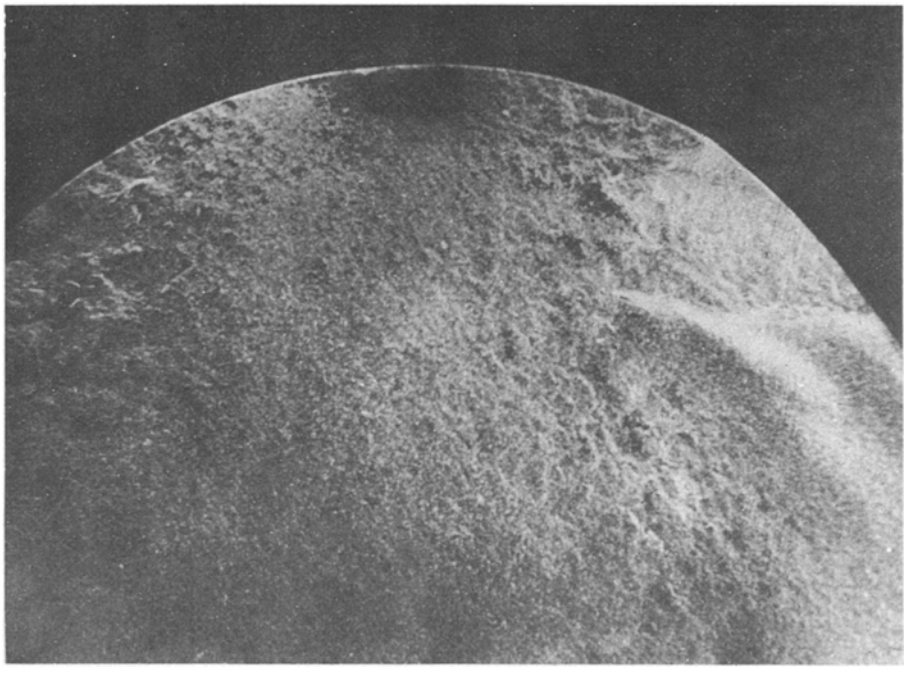

Figure 1 Hot-pressed alumina (specimen R-5) fractured by a linearly increasing load at 436 MPa (X 30).

were selected for investigation. The results are presented in the next section.

3. Results and discussion

3.1. Fractures at room temperature, normal loading rate

Fracture surface of a specimen fractured in flexure by a linearly increasing load at a fracture stress of 436 MPa is shown in Figs. 1 and 2. The fracture origin is a machining flaw about 15 to 20 μm deep. This flaw is bounded by a region of mainly transgranular fracture that appears as a dark spot at the top of the fracture surface in Fig. 1. At higher magnification in Fig. 2, the increase in transgranular fracture along the radius from the fracture origin, followed by a decrease in transgranular fracture, is evident. The K_I versus PIF curve for this specimen is given in Fig. 3. A horizontal dashed line indicates K_{IC} for the polycrystalline material. The minimum in PIF (maximum in percent transgranular fracture) almost coincides with K_{IC}.

3.2. Loading-rate dependence

Specimens fractured by delayed fracture and by impact were measured. The loading-rate variations were observed by comparing K_I versus PIF curves for delayed fracture, normal loading rate and impact fractures.

The K_{IC} versus PIF curve for a delayed fracture specimen fractured at 467 MPa in 362 sec is given in Fig. 4. This figure illustrates the increased detail observable in delayed fracture specimens. Again, there is a minimum in PIF near K_{IC}. Comparison of this curve with the previous one reveals another typical feature, a secondary minimum at about 5.6 MPa $m^{1/2}$. Overall, the minima in PIF in Fig. 4 occur at K_I values close to the K_{IC} values for various crystal lattice places as listed in Table 1.

There are definite differences between the curves in Fig. 3 and 4 at low values of K_I. In this region ($K_I < 2$ MPa $m^{1/2}$), the PIF depends on the type of flaw in each case. Machining flaws and surface pores have relatively high PIF. Large grains or groups of large grains acting as fracture origins tend to cleave, leading to relatively low values of PIF. When subsurface flaws are present, cleavage

TABLE I Fracture energies [9, 10] and critical stress intensity factors for several crystal-lattice planes in Sapphire

Fracture plane	Fracture energy ($J\,m^{-2}$)	Critical stress intensity factor (MPa $m^{1/2}$
1012	6.0	2.15 (1.7)*
1010	7.3	2.4
1126	24.4	4.3
0001	>40	>5.6

* See [10].

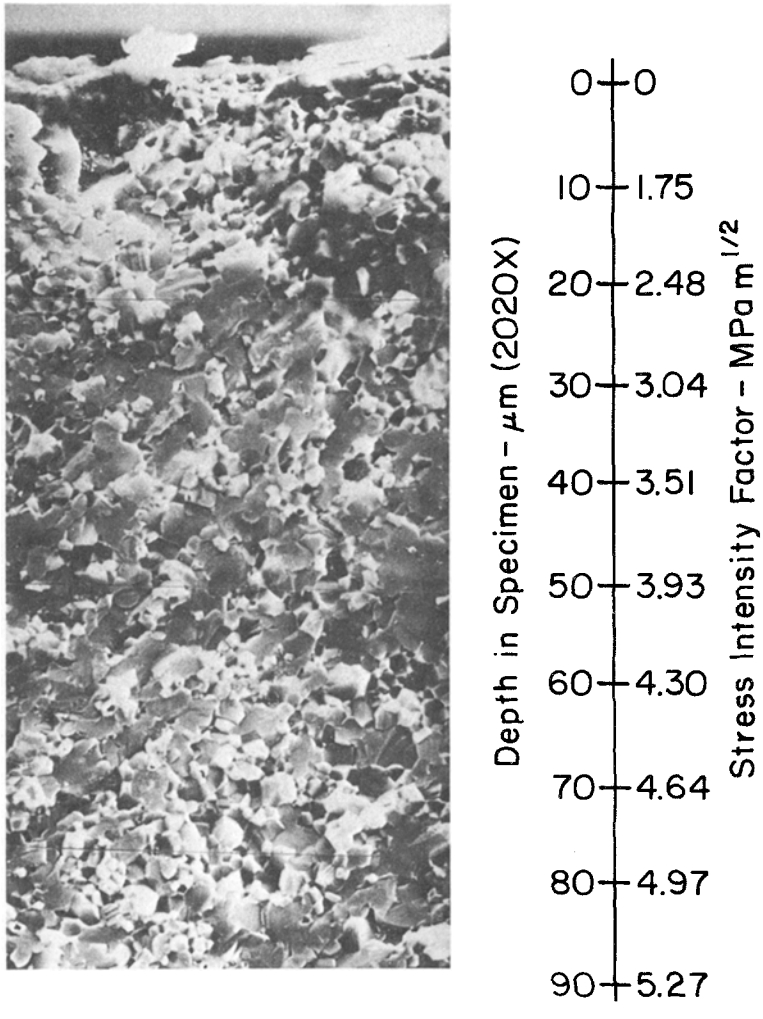

Figure 2 Hot-pressed alumina (specimen R-5) fractured by a linearly increasing load at 436 MPa (× 2020).

of the polycrystalline material between the flaw and the surface may indicate flaw linking [13] prior to fracture.

The K_I versus PIF curve for specimen I-18 fractured by impact is given in Fig. 5. The fracture stress is not measured directly during impact testing. Therefore, the fracture stress, necessary to compute K_I, was obtained from measurement of the fracture mirror radius using [14]

$$A = \sigma_F r_m^{1/2}$$

in which $A = 10.3$ MPa m$^{1/2}$ [15] and r_m is the fracture mirror radius. The resulting fracture stress was 841 MPa. At the high loading rates characteristic of impact fractures there is much less subcritical crack growth than there is in the specimens fractured at lower loading rates. As a result, the fracture stresses are higher and variations in PIF occur close to the fracture origin and are obscured to some degree by the transition from the flaw to the subcritical crack-growth region. These conditions result in a K_I versus PIF curve in which the minor fluctuations are absent or poorly defined. Despite this fact, a definite minimum in PIF was observed at K_I close to K_{IC} of the polycrystalline material.

3.3. Temperature dependence

Specimens fractured at elevated temperatures (800° C) were also measured. The results for a particular specimen (E-17), fractured at 528 MPa, are given in Fig. 6. There is more intergranular fracture at 800° C than at room temperature but the shape of the curve remains roughly the same showing a primary minimum and secondary minima. Because K_{IC} values at elevated tempera-

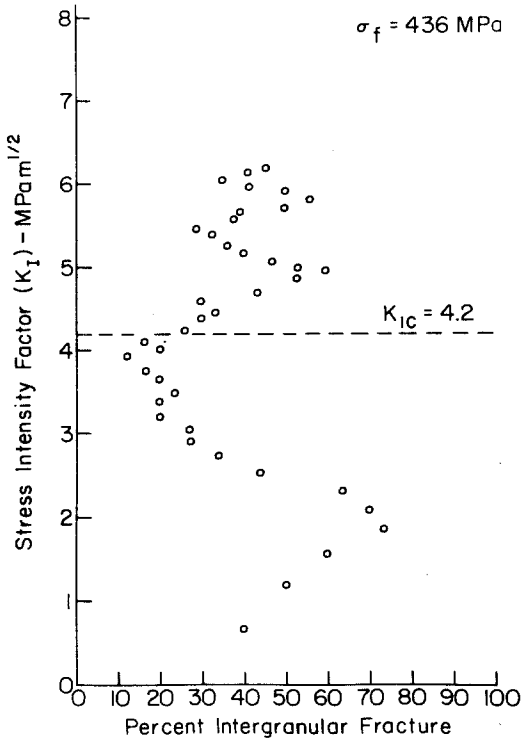

Figure 3 Stress intensity factor versus % intergranular fracture, linear loading rate (hot-pressed alumina, specimen R-5).

tures are not available it is not possible to compare K_I at minimum PIF with K_{IC}. However, if this K_I is taken as a criterion for the subcritical crack-growth boundary, the fact that this K_I is still in the same range indicates that K_{IC} has not changed very much.

Lankford [7, 8] indicates that twinning is more prevalent at elevated temperatures, that the twins are thicker, that there is multiple twin system activity, and that the onset of acoustic emission occurs at lower stresses. However, despite these facts, our observations indicate that there is less cleavage at high temperatures. Perhaps the increased thickness of the twins and increased multiple twin system activity allow accommodation of more strain without cleavage thus leading to the higher fracture stresses observed in the temperature range 500–1000° C [16].

3.4. Discussion

The fact that the K_I at the lowest minimum in PIF coincides approximately with K_{IC} of the polycrystalline body suggests that the minimum in PIF (or the maximum in % transgranular fracture) can be used as a criterion to locate the subcritical crack-growth boundary in fine-grained H-P alumina. Presumably, this criterion can be used to locate subcritical crack-growth boundaries in fractures for which the fracture stress was not measured, making it possible estimate the fracture stress and stress distribution in such specimens. Also, the information should be helpful for calculating branching radius to critical flaw size ratios more precisely than has been done in the past. Determination of these ratios for various materials is important for the theory of crack propagation. The fact that K_{IC} almost coincides with K_I at the minimum in PIF, and considering that, at room temperature, almost all of the fracture at the subcritical crack-growth boundary is transgranular suggests that critical crack growth begins when increased fracture energy can no longer be obsorbed by cleavage on these lattice planes.

Comparison of the K_I versus PIF curves with the K_{IC} values for the individual fracture events listed in Table I leads to interesting results. Based on the K_{IC} values for $\bar{1}012$ planes, one would expect crack growth to begin by cleavage on these planes of favourably oriented crystals at stresses of about 300 to 400 MPa (assuming a semicircular surface flaw with a radius of 20 μm). If the flaw is primarily intergranular, this will lead to decreasing

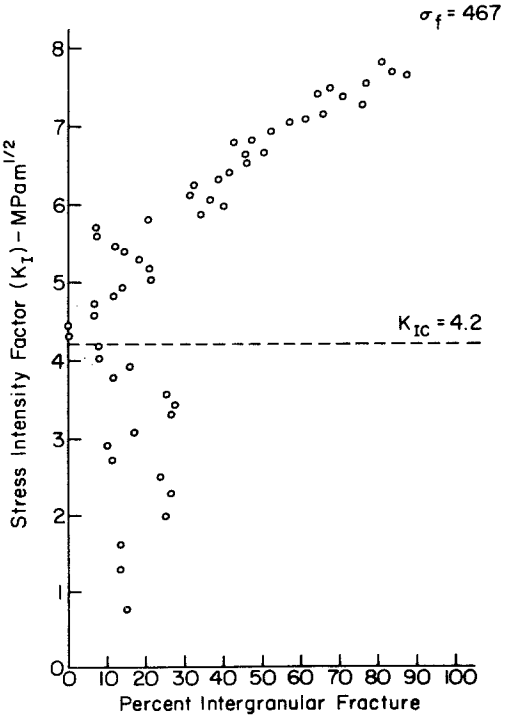

Figure 4 Stress intensity factor versus % intergranular fracture, delayed fracture (hot-pressed alumina, specimen D-12).

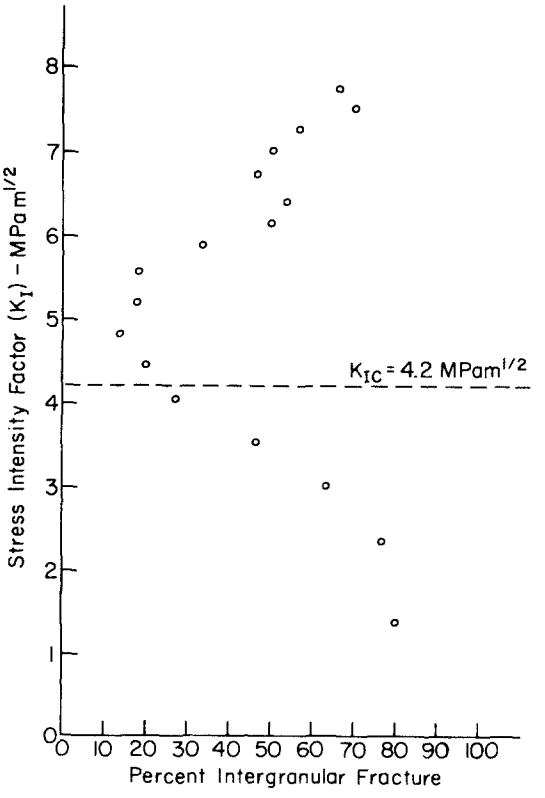

Figure 5 Stress intensity factor versus % intergranular fracture, impact loading (hot-pressed alumina, specimen I-18).

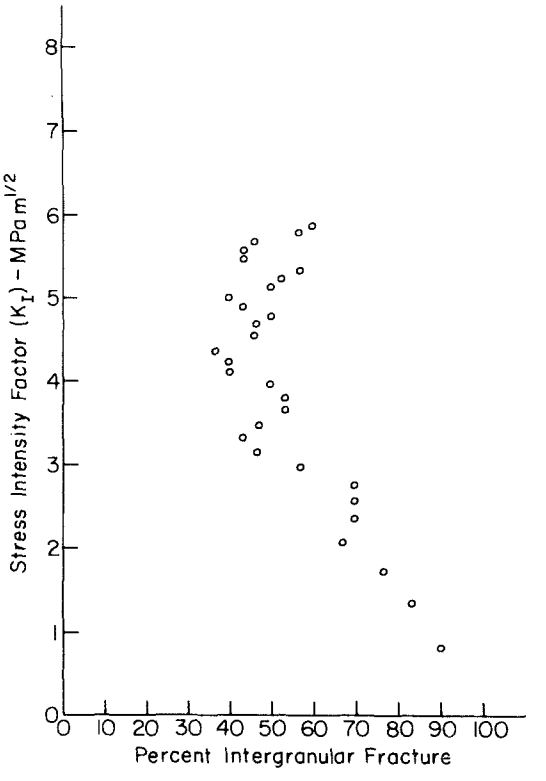

Figure 6 Stress intensity factor versus % intergranular fracture, linear loading rate at 800° C (hot-pressed alumina, specimen E-17).

PIF in the region surrounding the flaw (Fig. 3). Apparently, intergranular fracture can also occur at these low stresses, perhaps aided by stress intensification at cleaved grains or by stress corrosion. As the crack depth and K_I increase, cleavage on other planes becomes possible. This effect, plus the tendency for twinning to be propagated from one grain to the next, will cause further decrease in PIF. At $K_I = 4.3$ MPa m$^{1/2}$ where all of the planes with measured values of K_{IC}, except (0 0 0 1) can cleave the PIF is very low. Becher [12] has shown that basal twins induced by grinding cause small (0 0 0 1) fracture surfaces in sapphire indicating that fracture on (0 0 0 1) is possible even though it was not observed by Wiederhorn. However, twinning is a time-consuming process [8]. A long extrapolation of Lankford's acoustic emission data indicates that strain rates of about 10^8 sec^{-1} would be required to suppress twinning (on all planes). Very high strain rates are present at the tips of running cracks. Therefore, it is not surprising that, as the crack accelerates near K_{IC}, the cleavage mechanisms gradually drop out and PIF increases.

One can speculate that the increase in PIF just above $K_{IC} = 4.2$ MPa m$^{1/2}$ is limited by the increased availability of another cleavage mechanism as K_{IC} increases. This mechanism may be cleavage on $\{\bar{1}\,0\,1\,0\}$ combined with conchoidal fracture roughly parallel to $\{0\,1\,\bar{1}\,4\}$ which occurs because of the difficulty of (0 0 0 1) cleavage, as suggested by Wiederhorn [9]. In any case, the increase in PIF is reversed and with further increase in crack velocity and K_I, PIF passes through a secondary minimum at $K_I \cong 5.6$ MPa m$^{1/2}$. Above this value of K_I, PIF increases to high values (Fig. 4).

The technique described in this paper requires very precise location of the fracture origin. For example, in the early stages of the investigation, specimen R-45 ($\sigma_F = 660$ MPa) was assumed to have a fracture origin at the surface. The K_I versus PIF curve was determined and found to have a minimum in PIF at 6.6 MPa m$^{1/2}$, by far the highest value observed thus far for H-P, alumina. On re-examination, the actual fracture origin was found to be 19 μm below the surface. The K_I values were recalculated, assuming a subsurface

TABLE II Stress intensity factors* at minima % intergranular fracture in hot-pressed alumina

Specimen no.	Fracture stress (MPa)	K_I and (PIF) at minimum near $K_{IC} = 4.2\ MPa\ m^{1/2}$	K_I and (PIF) at minimum near $K_I = 5.6\ MPa\ m^{1/2}$	Comments
Delayed fracture specimens				
D-13	458	4.6 (21%)	5.7 (24%)	
D-12	467	4.3 (0%)	5.7 (7%)	
Linear loading-rate specimens				
R-5	436	4.0 (13%)	5.6 (29%)	
R-13	477	4.9 (17%)	6.2 (30%)	
R-15	494	4.9 (20%)	6.0 (13%)	Primary and secondary minima are interchanged
R-21	See comments			Results rejected because of uncertainty in fracture stress
R-45	660	4.8 (8%)	5.9 (11%)	Subsurface fracture origin
	Average	4.6 (13%)	5.85 (19%)	
Impact specimen				
I-18	841	4.8 (14%)	None	
Elevated Temperature specimens				
		K_I at minimum PIF		
E-17	528	4.3 (37%)		
E-11	461	3.9 (30%)		Subsurface fracture origin

* K_I calculated assuming a semi-circular flaw except for R-45 and E-11 for which an internal penny-shaped crack was assumed.

penny-shaped flaw. The minimum in PIF is at about $4.8\ MPa\ m^{1/2}$, a value that is now in the probable range of sample to sample variation of K_{IC}. Again, there is a secondary minimum at about $5.6\ MPa\ m^{1/2}$.

The stress intensity factors at the minima in PIF for the H-P alumina specimens investigated thus far are summarized in Table II. At room temperature the values of K_I at the lowest minimum in PIF near $K_{IC} = 4.2\ MPa\ m^{1/2}$ average $4.6\ MPa\ m^{1/2}$ and occur at an average of 13% intergranular fracture. The values of K_I at the secondary minimum in PIF near $K_I = 5.6\ MPa\ m^{1/2}$ average $5.85\ MPa\ m^{1/2}$ and occur at an average of 19% intergranular fracture.

In interpreting the above results it is important to realize that, first of all, the subcritical crack-growth boundary and K_{IC} do not coincide with the boundary of the region of reflecting spots which consistently falls at higher values of K_I. Secondly, although the cleavage tends to form a reflecting region, it tends to terminate in a region of primarily intergranular fracture. There is no evidence of microbranching in this region of intergranular fracture. Therefore, the region of reflecting spots is not exactly analogous to the mirror region in glass because in that case the mirror region terminates in a region of microbranching usually called mist.

The fact that PIF varies with K_I leads one to consider whether or not PIF can be used to roughly estimate K_I at points on the fracture surface other than close to the fracture origin. Some steps were taken to evaluate this possibility. A substantial reduction in stress intensity factor is expected in the region of crack branching. A preliminary examination of fracture surfaces just before and just after crack branching failed to reveal a substantial change in PIF. The fracture remained primarily intergranular. Therefore, one can conclude that K_I remains above K_{IC} during crack branching in H-P alumina. This result is consistent with the observation of Döll [17] who found that the crack velocity decreases only slightly from the maximum crack velocity during branching in glass.

In flexural specimens, K_I increases from the fracture origin to a maximum between 0.45 and 0.55 of the distance from the origin to the neutral axis [18, 19] and then decreases. K_I versus (a) curves extrapolate to $K_I = 0$ at about 1.4 to 1.6 of the distance from the origin to the neutral axis. Reflecting spots were observed at 1.2 of this distance. The area of reflecting spots was examined by SEM and was found to be caused by cleavage. Apparently, the stress intensity factor and crack velocity in this region were low enough so that the fracture was characterized by a distribution of

types of individual fracture events like that occurring during subcritical crack growth near the fracture origin.

Preliminary evaluations of K_I versus PIF curves for two other materials, 96% alumina and H-P Si_3N_4, indicate that different fracture mechanisms occur at subcritical crack-growth boundaries in these other materials. Therefore, one should expect different mechanisms and different criteria for the subcritical crack-growth boundary in various ceramic materials.

The fact that the frequencies of various individual fracture events at K_{IC} are different from those at crack branching has implications for theories of crack propagation. Clearly, if there is a variation in the frequencies of individual fracture events with K_I, the fracture energy varies with crack velocity. In comparing the fracture energies at criticality with those at crack branching, it is clear that, because there is no necessary relation between the distributions of the frequencies of the individual fracture events at criticality and at crack branching, there is no necessary relationship between fracture energies and thus no necessary relationship between K_{IC} and the stress intensity factor at crack branching (K_B). This result is important because it has been argued that there is a fixed ratio of crack-branching radius to critical flaw size in various materials [20, 21]. If this were correct it would imply that there is a direct proportionality between K_B and K_{IC} which would hold over a range of materials. However, it appears that this is not the case for the reasons given above.

The existence of correlations between K_{IC} and the types of individual fracture events occurring on the fracture surface, indicates some hope for development of improved methods of determination of K_{IC}. The best methods, currently in use, involve determination of the curve of crack velocity versus K_I, selection of some arbitrary crack velocity usually in the range 10^{-4} to 1 m sec^{-1}, and estimation of K_{IC} as the K_I value at this velocity. However, it is clear from the fractographic investigation described above that in H-P alumina the crack grows subcritically until K_I becomes high enough for increased intergranular fracture to occur. Then, the structure "lets go" and failure occurs. In other materials the mechanisms may vary but they should be indentifiable. Therefore, it may be desirable to define K_{IC} in terms of the change in the types of individual fracture events rather than in terms of an arbitrary crack velocity.

4. Conclusions

(1) The variations of PIF with K_I confirm that there is a relationship between the K_{IC} values of the individual fracture events and the types of fracture events occurring in H-P alumina at particular values of K_I.

(2) The subcritical crack-growth boundary in H-P alumina occurs near the lowest minimum in PIF (the maximum in transgranular fracture).

Acknowledgements

The authors are pleased to acknowledge the contributions of their associates at Ceramic Finishing Company. This research was sponsored by the Naval Air System Command under Contract N00019-77-C-0328.

References

1. H. P. KIRCHNER, W. R. BUESSEM, R. M. GRUVER, D. R. PLATTS and R. E. WALKER, Ceramic Finishing Company Summary Report, Contract N00019-70-C-0418, December (1970).
2. H. P. KIRCHNER, R. M. GRUVER and R. E. WALKER, *J. Amer. Ceram. Soc.* 56 (1973) 17.
3. H. P. KIRCHNER and R. M GRUVER, *Phil. Mag.* 27 (1973) 1433.
4. R. M. GRUVER, W. A. SOTTER and H. P. KIRCHNER, Ceramic Finishing Company Summary Report, Contract N00019-73-C-0356 November (1974).
5. H. P. KIRCHNER, R. M. GRUVER and W. A. SOTTER, *Mat. Sci. Eng.* 22 (1976) 147.
6. J. LANKFORD, *J. Mater. Sci.* 12 (1977) 791.
7. J. LANKFORD, JUN., Southwest Research Institute Technical Report, Contract N00014-75-C-0668 April (1977).
8. *Idem,* "Compressive Microfracture and Indentation Damage in Alumina", in "Fracture Mechanics of Ceramics", Vol. 3, edited by R. C. Bradt, D. P. H. Hasselman and F.F. Lange (Plenum, New York, 1978).
9. S. M. WIEDERHORN, *J. Amer. Ceram. Soc.* 52 (1969) 485.
10. *Idem,* "Subcritical Crack Growth in Ceramics", in "Fracture Mechanics of Ceramics", Vol. 2, edited by R. C. Bradt, D. P. H. Hasselman and F. F. Lange (Plenum, New York, 1974) pp. 613–46.
11. G. K. BANSAL and W. H. DUCKWORTH, "Effects of Specimen Size on Ceramic Strengths", in "Fracture Mechanics of Ceramics", Vol. 3, edited by R. C. Bradt, D. P. H. Hasselman and F. F. Lange (Plenum, New York, 1978) p. 190.

12. P. F. BECHER, *J. Amer. Ceram. Soc.* **59** (1976) 59.
13. A. G. EVANS and G. TAPPIN, *Proc. Brit. Ceram. Soc.* **20** (1972) 276.
14. H. P. KIRCHNER, R. M. GRUVER and W. A. SOTTER, *J. Amer. Ceram. Soc.* **58** (1975) 188.
15. H. P. KIRCHNER, *Eng. Fract. Mech.* **10** (1978) 283.
16. H. P. KIRCHNER and R. M. GRUVER, *Mat. Sci. Eng.* **13** (1974) 63.
17. W. DÖLL, *Int. J. Fracture* **11** (1975) 184.
18. F. W. SMITH, A. F. EMERY and A. S. KOBAYASHI, *J. Appl. Mech. Series E* **34** (1967) 953.
19. H. P. KIRCHNER and J. W. KIRCHNER, *J. Amer. Ceram. Soc.* **62** (1979) 198.
20. J. J. MECHOLSKY, S. W. FREIMAN and R. W. RICE, *J. Mater. Sci.* **11** (1976) 1310.
21. G. K. BANSAL and W. H. DUCKWORTH, *J. Amer. Ceram. Soc.* **60** (1977) 304.

Received 6 October and accepted 18 December 1978.